7. Zhitomirsky, M. E., Rice, T. M. & Anisimov, V. I. Preprint cond-mat/9904330 at <http://xxx.lanl.gov> (1999).
8. Tinkham, M. *Introduction to Superconductivity* (McGraw Hill, New York, 1996).

Developmental biology

Variable cell number in nematodes

Studies of the nematode worm *Caenorhabditis elegans* have led to the widely held belief that individuals of a given nematode species are characterized by a property known as eutely, in which all individuals have the same total number of cells[1]. This property, which is peculiar to nematodes and a few other phyla, has raised the question of whether the developmental mechanisms of nematodes differ from those of larger metazoans. Here we show that many, perhaps most, nematode species are not eutelic in at least one organ, the epidermis, and that in this respect they resemble other model organisms such as fruitflies and mice.

Although most *C. elegans* cell lineages are invariant, a few are not (such as intestinal lineages)[2–4]. Limited cell-lineage variation has also been found in other species of nematode[5–8]: for example, in *Pelodera strongyloides*, the ventral epidermal cells P3.p and P9.p divide in about half the females[7]. To test whether a variable cell number is more widespread than such isolated cases suggest, we determined the among-individual variance (V_i) of epidermal nuclear number in adults of 13 species of free-living nematode from three families (Cephalobidae, Panagrolaimidae and Rhabditidae), which between them span the range in adult body size and adult epidermal cell number typical of free-living terrestrial nematodes (Fig. 1a). All these species have epidermal syncytia containing nuclei produced by a series of lateral seam cells that stop proliferating before adulthood.

V_i for epidermal nuclear number in *C. elegans* is not significant (likelihood ratio test, $P > 0.05$). This is to be expected, as there are no reports of variation in lateral-seam-cell lineages[2]. Four other species (*Caenorhabditis* sp. PS1010, *Oscheius myriophila*, *Panagrolaimus rigidus* and *Rhabditella octopleura*) do not deviate significantly from eutely. The remaining eight species show significant V_i for nuclear number, with *Panagrellus redivivus*, *Pellioditis* sp. EM434 and *Rhabditoides regina* having $V_i > 100$ (Fig. 1b).

Among species, V_i increases with the number of epidermal nuclei, N (Spearman's rank correlation, $\rho = 0.84$, $P < 0.001$; Fig. 1b). This relationship has evolved many times (regression through the origin of phylogenetically independent contrasts, assuming that branch lengths are equal[9], $\log V_i = 3.38 \log N$; $P = 0.006$). Body length (L) also increases with the number of nuclei ($\rho = 0.73$, $P = 0.004$; Fig. 1c), and this relationship has also evolved repeatedly ($\log L = 0.514 \log N$; $P = 0.003$). However, the relationship between V_i and body length is only weakly positive ($\rho = 0.59$, $P = 0.03$) and disappears after correcting for phylogeny ($\log V_i = 3.27 \log L$; $P > 0.1$). Reproductive mode (parthenogenetic, hermaphroditic and gonochoristic) does not have a significant effect on any of the traits studied ($P > 0.1$).

The evolution of V_i must be caused by changes in lateral-seam-cell lineages. We have modelled the V-cell lineages of *C. elegans*, *P. redivivus*, *R. octopleura* and *O. myriophila*[2,5,10] as discrete-time multitype branching processes and determined the resulting distribution of epidermal nuclear counts by simulation[10].

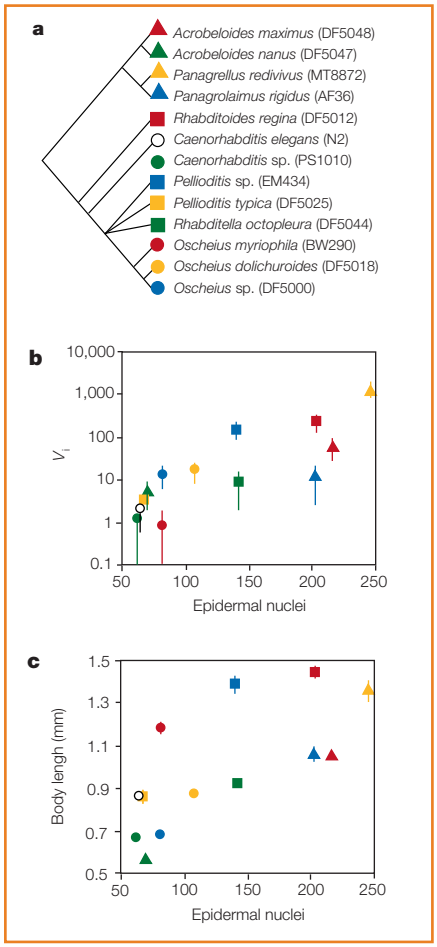

Figure 1 Relationship between body length, the number of epidermal nuclei and the among-individual variance in 13 nematode species. Lateral epidermal nuclei were independently counted 2–3 times (to account for measurement error) on one side of 10–14 early adult females or hermaphrodites from each species. For each species, among-individual variance (V_i) was estimated by maximum likelihood using a random effects one-way linear model. **a,** Phylogeny of the species studied (strain names in parentheses)[12,13]. *Acrobeloides* species are parthenogenic; the rest are gonochoristic, except *C. elegans*, *O. myriophila* and *Oscheius* sp. DF5000, which are hermaphroditic. **b,** Plot of V_i (log scale) against number of epidermal nuclei, *N*. **c,** Plot of body length against *N*. Error bars show standard errors.

The simulations suggest two reasons why species with many nuclei may be more variable than those with fewer[10]. First, V_i increases with the probability of deviating from the species' canonical lineage. Second, for a given probability of lineage variation, more complex lineages yield a higher V_i than simpler lineages. We conclude that the high observed value of V_i for *P. redivivus* results not only from the complexity of its lineage, but also from a greater propensity to deviate from the canonical lineage compared with the other species[10]. This is consistent with observations of variability in the V-cell lineages of *P. redivivus* [5] and *R. regina*, which have high V_i values. Loss of hypodermal eutely also occurs in several species of primitive marine nematode that have a cellular, rather than syncitial, hypodermis[11].

Given that the terrestrial free-living nematodes studied here are smaller and have fewer epidermal nuclei than most marine and animal parasitic nematodes, it is likely that most nematode species are not eutelic and so resemble other metazoans.

Ana Cunha*, Ricardo B. R. Azevedo*, Scott W. Emmons†, Armand M. Leroi*
**Department of Biology, Imperial College, Silwood Park, Ascot, Berkshire SL5 7PY, UK*
e-mail: a.leroi@ic.ac.uk
†Department of Molecular Genetics, Albert Einstein College of Medicine, Bronx, New York 10461, USA

1. Van Cleave, H. J. *Q. Rev. Biol.* **7,** 59–67 (1932).
2. Sulston, J. E. & Horvitz, H. R. *Dev. Biol.* **56,** 110–156 (1977).
3. Sulston, J. E. *et al. Dev. Biol.* **100,** 64–119 (1983).
4. Kimble, J. & Hirsh, D. *Dev. Biol.* **70,** 396–417 (1979).
5. Sternberg, P. W. & Horvitz, H. R. *Dev. Biol.* **93,** 181–205 (1982).
6. Ambros, V. & Fixsen, W. in *Development as an Evolutionary Process* (eds Raff, R. A. & Raff, E. C.) 139–159 (Liss, New York, 1987).
7. Sommer, R. J., Carta, L. K. & Sternberg, P. W. *Development* **120,** 85–95 (1994).
8. Voronov, D. A. & Panchin, Y. V. *Development* **125,** 143–150 (1998).
9. Purvis, A. & Rambaut, A. *Comput. Appl. Biosci.* **11,** 247–251 (1995).
10. Azevedo, R. B. R. *et al. Nematology* (in the press).
11. Rusin, L. U. R. & Malakov, V. V. *Doklady Biol. Sci.* **361,** 331–333 (1998).
12. Fitch, D. H., Bugaj-Gaweda, B. & Emmons, S. W. *Mol. Biol. Evol.* **12,** 346–358 (1995).
13. Blaxter, M. L. *et al. Nature* **392,** 71–75 (1998).

Nanoelectronics

Growing Y-junction carbon nanotubes

The synthesis of connections between two or more different carbon nanotubes is an important step in the development of carbon nanotube-based electronic devices and circuits[1–4]. But this is difficult to achieve using conventional methods to grow carbon nanotubes[5] because the straight tube structure cannot be controllably altered along its length. Various ideas for post-growth modifications have been suggested[6],

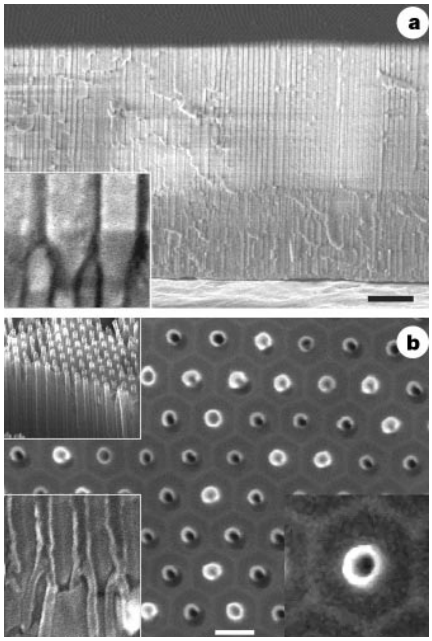

Figure 1 Controlled growth of Y-junction nanotubes. **a,** SEM image of Y-branched nanochannel template (scale bar, 1 μm). The template was formed by first anodizing a sheet of high-purity aluminium in 0.3 M oxalic acid at 10 °C under a constant voltage of 50 V for 15 h, resulting in a hexagonal array of pores near the aluminium surface[11]. After chemically removing the original film, a second anodization was performed under the same conditions, typically for 30 min. The anodization voltage was then reduced to about 35 V. Because the pore cell diameter is proportional to the anodization voltage[12,13], reducing the voltage by a factor of $1/\sqrt{2}$ results in twice as many pores appearing in order to maintain the original total area of the template, and nearly all pores branched into two smaller-diameter pores. The resulting template consists of parallel Y-branched pores with stems 40 nm in diameter and branches 28 nm in diameter. The arrow shows where Y branches start to grow (see inset for close-up). **b,** Top-view SEM image of carbon nanotubes aligned in the template after ion-milling of amorphous carbon on the surface (scale bar, 100 nm). The nanotube diameter is larger than the original pore owing to thermal expansion of the template during growth. Top inset, stem part of the Y-junction tubes. Bottom left inset, close-up of the region between stem and branch portions still embedded in the template. Bottom right inset, close-up of the top of the nanotube in its hexagonal cell.

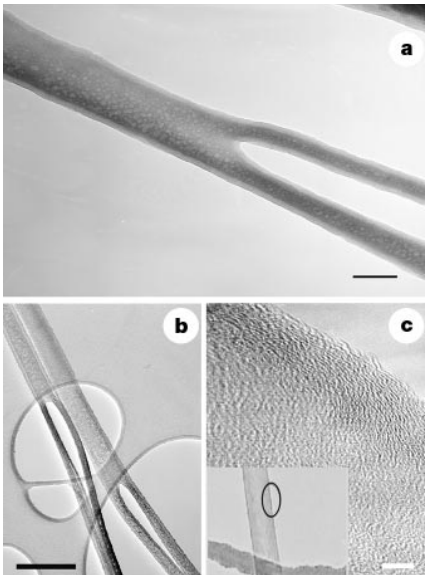

Figure 2 TEM images of Y-junction nanotubes. **a,** Y-junction tube (scale bar, 50 nm) with stem ~90 nm and branches 50 nm in diameter. The interior of the tube contains some residual amorphous carbon which can be reduced by optimizing growth conditions[14]. **b,** Y-junction formed by using higher anodization voltages, resulting in stems ~100 nm and branches 60 nm in diameter (scale bar, 200 nm). **c,** High-resolution TEM image of typical Y-junction nanotube wall showing graphitic multi-wall structure (scale bar, 5 nm). Inset, the part of the tube that was imaged; the dark object in the background is part of the holey-carbon TEM grid.

but these have been hard to implement and are prone to defects. Here we use nanostructured template channels to grow individual Y-junction carbon-nanotube heterostructures by the pyrolysis of acetylene with cobalt catalysis.

Our approach to growing individual Y-junction nanotubes is based on nanochannel alumina (NCA) template growth, which was previously used in the synthesis of various nanostructures[7], including straight carbon nanotubes[8,9] and their highly ordered arrays[10]. We extended the NCA template method to grow Y-junction carbon nanotubes by first forming a Y-branched nanochannel template (Fig.1a). We then electrochemically deposited a small amount of cobalt catalyst in the bottom of the template channels and reduced the catalyst at 600 °C for 4–5 hours under a carbon monoxide flow (100 cm^3 min^{-1})[10]. The Y-junction nanotubes are then grown by pyrolysis of acetylene at 650 °C. We discuss here our initial results on growing Y-junction nanotubes; a more detailed description of the fabrication process will be presented elsewhere.

The scanning electron microscope (SEM; HS-4500) image in Fig. 1a shows the cross-section of a typical Y-branched template consisting of 'stems' 3 μm long and 'branches' 2 μm long. All the branching occurs at the same depth, as indicated by the arrow. The SEM image in Fig. 1b shows a top view of the branched NCA template after pyrolytic nanotube growth consisting of nanotubes 60 nm in diameter arranged in a hexagonal lateral superlattice with a density of about 10^9 cm^{-2}.

The top inset shows the length of the stems after partly exposing the template using a chemical etch. The bottom inset shows a cross-section of the branching point of the Y-junction tubes embedded in the template, with the larger carbon nanotube (stem) gradually evolving into two branches 35 nm in diameter, forming a continuous Y junction with three clearly separated ports. The Y junctions are uniform with regard to the position of the junction and the diameter of the arms.

We further characterized the Y-junction nanotubes by using transmission electron microscopy (TEM; H-7000 or JEOL-2021F) after removing the tubes from the NCA template. By varying the anodization conditions, we were able to produce Y-junction nanotubes with stems and branches of different diameters (Fig. 2a,b). High-resolution TEM images of the tube walls (Fig. 2c) and electron-diffraction patterns of the tubes show that both the stem and the branched portions have a graphitic multi-walled structure up to a few nanometres thick (depending on the diameter), similar to that of straight nanotubes grown using pyrolytic methods[8–10].

Y-junction carbon nanotubes can therefore be grown controllably and in preference to straight nanotubes. Although straight nanotubes have previously been grown by pyrolysis within NCA templates, our use of individual Y-branched channels to grow three-terminal nanotubes involves a more complex growth mechanism that is yet to be determined. It is likely that, by confining the nanotube to grow within a Y-branched channel, we are effectively placing a constraint on the catalytic decomposition of acetylene, forcing the tube structure to grow along the channel wall, which also acts as a weak catalyst[10].

Using a Y-branched nanochannel for pyrolytic nanotube growth allows the formation of large numbers of well-aligned Y-junction carbon nanotubes, with excellent uniformity and control over the length (up to several tens of micrometres) and diameter (15–100 nm) of the stem and branches. These Y junctions provide the nanoelectronics community with a new base material for the development of molecular-scale electronic devices.

Jing Li, Chris Papadopoulos, Jimmy Xu*
Department of Electrical and Computer Engineering, University of Toronto, 10 King's College Road, Toronto, Ontario M5S 3G4, Canada
**Present address: Division of Engineering, Brown University, Providence, Rhode Island 02912, USA*
e-mail: jimmy_xu@brown.edu

1. McEuen, P. L. *Nature* **393,** 15–17 (1998).
2. Kouwenhoven, L. *Science* **275,** 1896–1897 (1997).
3. Chico, L., Crespi, V. H., Benedict, L. X., Louie, S. G. & Cohen, M. L. *Phys. Rev. Lett.* **76,** 971–974 (1996).
4. Mennon, M. & Srivastava, D. *Phys. Rev. Lett.* **79,** 4453–4456 (1997).
5. Ebbsen, T. W. *Carbon Nanotubes: Preparation and Properties* (CRC Press, Boca Raton, Florida, 1997).
6. Collins, P. G., Bando, H. & Zettl, A. *Nanotechnology* **9,** 153–157 (1998).
7. Routkevitch, D. *et al. IEEE Trans. Electron. Devices* **43,** 1646–1658 (1996).
8. Kyotani, T., Tsai, L. & Tomita, A. *Chem. Mater.* **8,** 2109–2113 (1996).
9. Che, G., Lakshimi, B., Martin, C. R., Fisher, E. R. & Ruoff, R. S. *Chem. Mater.* **10,** 260–267 (1998).
10. Li, J., Papadopoulos, C. & Xu, J. M. *Appl. Phys. Lett.* **75,** 367–369 (1999).
11. Masuda, H. & Fukuda, K. *Science* **268,** 1466–1468 (1995).
12. O' Sullivan, J. P. & Wood, G. C. *Proc. R. Soc. Lond. A* **317,** 511–543 (1970).
13. Broughton, J. & Davies, G. A. *J. Membr. Sci.* **106,** 89–101 (1995).
14. Baker, R. T. K., Chludzinski, J. J. Jr & Lund, C. R. F. *Carbon* **21,** 295–303 (1987).